ACS Photonics

Article

pubs.acs.org/journal/apchd5

Strong Magnetochiral Dichroism in Suspensions of Magnetoplasmonic Nanohelices

Vassilios Yannopapas*,† and Alexandros G. Vanakaras‡

†Department of Physics, National Technical University of Athens, GR-15780 Athens, Greece

‡Department of Materials Science, School of Natural Sciences, University of Patras, Patras 265 04, Greece

Supporting Information

ABSTRACT: We show theoretically that self-assembled metamaterial suspensions of magnetoplasmonic entities in the form of magnetic-nanoparticle helices coiled around plasmonic (gold) nanorods exhibit very strong magnetochiral dichroism that is orders of magnitude higher than in conventional materials exhibiting this phenomenon (liquid molecular systems, anisotropic crystals, and chiral ferromagnets). The large values of the calculated magnetochirality are accompanied by an enhancement of the magneto-optical Faraday effect due to the excitation of surface plasmons at the nanorods as well as by an increase of the structural dichroism imparted from the helicoidal arrangement of the magnetic nanoparticles. However, the reported enhancement of the magnetochiral dichroism does not appear to be a cascade phenomenon of the structural and magnetic circular dichroism as, for example, in solutions of magnetic compounds, but appears as a possible manifestation of the emergence of a surface-plasmon-induced toroidal moment within the nanoparticle helices. To the best of our knowledge, it is the first time that the presence of a toroidal moment in a material can exhibit significant reciprocity-violating anisotropy in the optical regime.

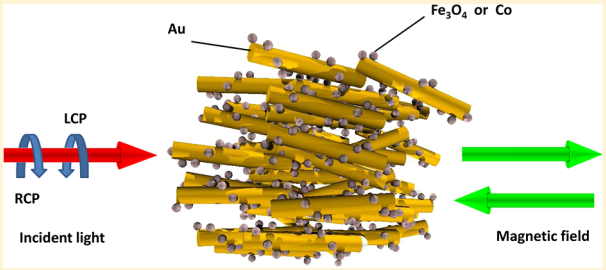

KEYWORDS: *magnetic nanoparticles, circular dichroism, magnetochiral effect, Faraday rotation, magneto-optical effect, surface plasmons*

Magnetochirality is a term encompassing phenomena related with electromagnetic (EM)-wave propagation in chiral substances or structures under the influence of an external, static magnetic field. Such phenomena are birefringence in EM wave refraction or dichroism in wave absorption stemming from a small shift in the material refractive index.[1] The presence of an external magnetic field within a chiral medium means the occurrence of time-reversal as well as space-reversal symmetry breaking simultaneously, being distinct from reciprocal phenomena by the presence of only geometrical chirality or a magnetic field. As a second-order phenomenon, magnetochirality is very hard to measure experimentally and has so far been verified in liquid molecular systems, organic compounds, anisotropic crystals, and chiral ferromagnets.[2−13] Very recently, it has been theoretically suggested that magnetochiral dichroism (MChD) can be promoted in chiral magnetic metamaterials such as helical lattices of magnetic garnet spheres.[14] Furthermore, in a very recent experiment it has been demonstrated that chiral magnetic nanohelices exhibit strong MChD in the optical regime.[15] In the present work we demonstrate that the MChD effect can be even more enhanced by several orders of magnitude if *magnetic* in conjunction with *plasmonic* materials are used for realizing *magnetoplasmonic* helical structures.

Surface plasmons (SPs) are EM waves coupled to the collective oscillations of the electrons in an interface between two media with permittivities with opposite sign, typically a dielectric and a metal. Localized SPs, also called particle plasmons, are plasma oscillations occurring at the surface of a finite nano-object, i.e., a sphere or a rod. One of the salient features of metallic nanostructures supporting SPs is their ability to manipulate and localize light in volumes that are much smaller than the wavelength, i.e., in subwavelength volumes, rendering them as ideal candidates for nanophotonic devices. The strong confinement of light in subwavelength volumes results in huge values of the local field, boosting the impact of a plethora of phenomena and properties such as Raman scattering, nonlinearities, and light−matter interactions, to name a few. Among these phenomena that are promoted by SP excitations are the magneto-optical phenomena such as the Kerr and Faraday effects, which take place in nanostructures combining magnetic and plasmonic functionalities.[16−35]

As stated above, MChD is a cross effect and takes place in systems containing both natural circular dichroism (NCD) and magnetic circular dichroism (MCD). As such, it is worth examining whether MChD can be boosted with the assistance of SPs, which enhance the magneto-optical (MO) effect. In this respect, we present a system containing magnetic and plasmonic materials arranged in a chiral fashion, aiming at achieving strong magnetochiral dichroism. Namely, we consider a collection (suspension) of randomly oriented helices of

Received: January 29, 2015
Published: June 26, 2015

DOI: 10.1021/acsphotonics.5b00237
ACS Photonics 2015, 2, 1030−1038

magnetic nanoparticles coiled around a noble-metal nanorod (in our case a gold nanorod), under an external static magnetic field. We find, in particular, that the SP-induced strong localization of the EM field within the magnetic NPs enhances the MCD and the MChD by several orders of magnitude.

MAGNETOCHIRAL DICHROISM

The dielectric tensor of a homogeneous chiral medium subject to a magnetic field **B**, to first order in wavevector **k** and **B**, is written as[3]

$$\epsilon_{\pm}^{\mathrm{L,R}}(\omega, \mathbf{k}, \mathbf{B}) = \epsilon_0(\omega) \pm \alpha_{\mathrm{NCD}}^{\mathrm{L,R}}(\omega)k \pm \beta_{\mathrm{MCD}}(\omega)B + \gamma_{\mathrm{MChD}}^{\mathrm{L,R}}(\omega)\mathbf{k}\cdot\mathbf{B} \quad (1)$$

where the symbol L indicates left-circularly polarized (LCP) and R indicates right-circularly polarized (RCP) light. $\alpha_{\mathrm{NCD}}^{\mathrm{L,R}}k$ is the NCD contribution (in the absence of magnetic field, i.e., $\mathbf{B} = 0$), $\beta_{\mathrm{MCD}}(\omega)B$ is the contribution of MCD (Faraday effect), and the third term, $\gamma_{\mathrm{MChD}}^{\mathrm{L,R}}(\omega)\mathbf{k}\cdot\mathbf{B}$, corresponds to the MChD effect taking place in the presence of a magnetic field acting on a chiral medium. The MChD term depends on the relative orientation of the wavevector **k** and the magnetic field **B** and on the sense of handedness of the chiral medium, while being independent of the polarization of incident light (MChD occurs for unpolarized incident light). The above three effects are substantiated via the measurement of absorption circular dichroism (CD) for LCP and RCP incident light, i.e.,

$$\mathrm{CD} = 2\frac{A_{\mathrm{RCP}} - A_{\mathrm{LCP}}}{A_{\mathrm{RCP}} + A_{\mathrm{LCP}}} \quad (2)$$

$$\mathrm{NCD} = \mathrm{CD}(\mathbf{B} = 0) \quad (3)$$

$$\mathrm{MCD} = \mathrm{CD}(\mathbf{B}) - \mathrm{NCD} \quad (4)$$

$$\mathrm{MChD} = A(\mathbf{k} \uparrow \uparrow \mathbf{B}) - A(\mathbf{k} \uparrow \downarrow \mathbf{B}) \quad (5)$$

where A in the last of the above equations is the absorbance for unpolarized light, i.e., $A = (A_{\mathrm{RCP}} + A_{\mathrm{LCP}})/2$.

When the real part of the dielectric tensor of eq 1 is much larger than its imaginary part, then MChD $\approx$ (NCD) $\times$ (MCD), verifying the cross-effect nature of MChD.[3] As such, MChD is expected to be strong in systems having substantial NCD and MCD. Next, we present a composite MChD medium, i.e., a chiral magnetoplasmonic system, in an attempt to mimic the dielectric tensor of eq 1 for a homogeneous chiral medium but with values of γ_{MChD} that can be probed experimentally.

DESCRIPTION OF THE MAGNETOPLASMONIC METAMATERIAL

Our case study includes the suspensions depicted in Figure 1. They consist of gold (plasmonic material) nanorods around which are twice wound helices of magnetic NPs. The magnetic NPs have a 5 nm radius, while the gold nanorods have height h = 140 nm and diameter d = 10 nm. For dilute suspensions (under small pressure), the helices@nanorods are randomly oriented (top panel of Figure 1), while for dense suspensions (under large pressure) the helices@nanorods point, on average, in the same direction (bottom panel) in resemblance to the molecular orientation in nematic liquid crystals. The conformations of Figure 1 are determined by classical Monte Carlo simulations.

Figure 1. A dilute (f = 0.5%, top panel) and a dense (f = 14%, bottom panel) suspension of randomly oriented magnetic-NP helices coiled around a metallic nanorod (core). The dilute suspension (top panel) is an isotropic disordered mixture, while the dense (bottom panel) suspension exhibits a nematic liquid-crystalline-like order.

We note that metamaterial suspensions such as those depicted in Figure 1 have been realized with metallic NPs via bottom-up processes such as supramolecular self-assembly[36−38] as well as peptide- and DNA-assisted self-assembly[39−44] showing very high values of NCD thanks to the synergy of the chiral arrangement of the NPs with the excitation of SPs.[45−55]

The EM modeling of the suspensions of Figure 1 is performed via the discrete-dipole approximation (DDA) technique[56−58] for MO targets (scatterers).[59,60] An analytic description of the method is provided in the Supporting Information. In the calculations that follow, as magnetic NPs we have considered either magnetite or cobalt NPs, whose dielectric tensors are taken from experimental measurements of bulk magnetite[61,62] and cobalt.[21] The DDA method is employed for suspension samples of 36 helices@gold nanorods where each helix contains 12 magnetic (either cobalt or magnetite) NPs and is coiled twice around a gold nanorod. The DDA absorption cross sections A_{LCP} and A_{RCP} are calculated by averaging over 10 different sample configurations of 36 helices@nanorods. The corresponding azimuth and ellipticity rotation angles are calculated as the real and imaginary part, respectively, of the difference in the extinction coefficients between LCP and RCP incident light (see eqs 17−19 in the Supporting Information).

RESULTS AND DISCUSSION

To begin with, we assume that the gold nanorods are absent and the helices stand alone in space (see inset of Figure 2). Figure 2 shows the azimuth and ellipticity rotation angles (a), CD (b), MCD (c), and MChD (d) for a suspension of helices of magnetite NPs with f = 0.03% volume filling fraction. Light is incident along the z-axis ($\mathbf{k} = k_z\hat{z}$), while an external magnetic

DOI: 10.1021/acsphotonics.5b00237
ACS Photonics 2015, 2, 1030−1038

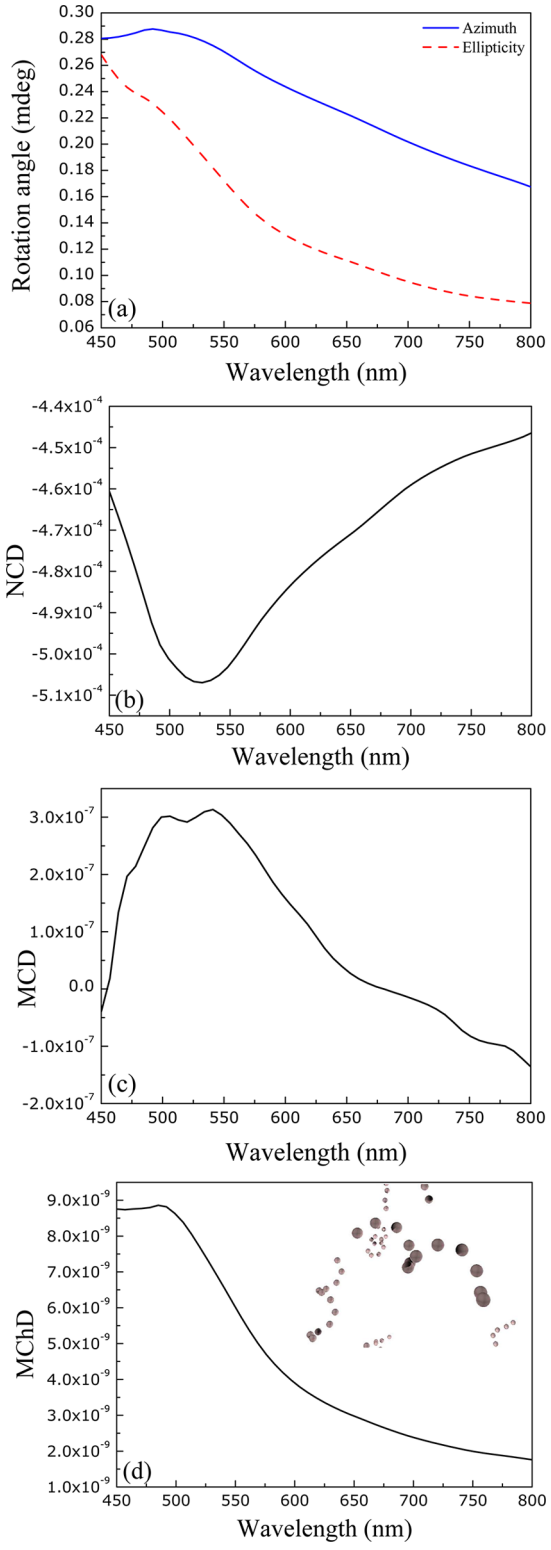

Figure 2. (a) Azimuth and ellipticity rotation angle for light incident along the positive z-axis at a suspension of 5 nm magnetite nanospheres forming helices coiled two times around a (void) cylinder with height h = 140 nm and diameter d = 10 nm; that is, the solution consists solely of magnetite NP helices with pitch $p = h/2$ = 70 nm and volume density f = 0.03% (see inset of part d). (b) Spectrum of natural dichroism (zero magnetic field) NCD. (c and d) Corresponding spectra for the magnetic (MCD) and magnetochiral (MChD) dichroism, respectively, for a magnetic field of 0.5 T along the positive z-axis.

field B = 0.5 T is applied either parallel or antiparallel to the incident wavevector **k**. We observe that both rotation angles are on the order of a fraction of a millidegree, while (the absolute values of) NCD and MCD exhibit maxima in the spectral region from 500 to 550 nm. MChD is very weak (on the order of 10^{-9}) and presents a local maximum around 510 nm. By inserting the gold core (nanorod) inside the magnetic nanohelices (see Figure 3), all quantities increase dramatically. The azimuth and ellipticity rotation angles increase by about 4 orders of magnitude, NCD increases by about 2 orders of magnitude, MCD increases by 2 orders of magnitude, and MChD increases by more than 6 orders of magnitude. As the MO rotation angles induced by a magnetic nanoparticle depend on the electric field concentrated within the volume of the magnetic NP,[63,64] upon excitation of a SP in a nearby noble-metal NP (in our case a gold nanorod; see Figure S1 of the Supporting Information material), the electric field within the magnetic NP is significantly enhanced, leading to more pronounced MO effects (it does not matter whether the gold and magnetic NPs are in contact or not as long as the electric field emitted by the SP excitation reaches the magnetic NP[18]). The plasmon-induced enhancement of the MO effect (MCD and rotation angles) promotes the calculated giant enhancement of the MChD (if MChD, to a first approximation, is viewed as a cascade of MCD and NCD).

In Figure 4 and Figure 5 we consider the same samples as those of Figure 2 and Figure 3 but for helices of cobalt NPs. In the absence of the gold core (nanorod), the standalone cobalt nanohelices exhibit rotation angles, MCD, and MChD increased by about 1 order of magnitude compared to the case of magnetite helices. This is more or less expected, as the MO (off-diagonal) components (Voigt parameter) of the dielectric tensor of bulk cobalt[21] are at least 1 order of magnitude larger than those of bulk magnetite[62] (see Figure S3 of the Supporting Information). The NCD spectra of both types of nanohelices (magnetite and cobalt) are on the same order of magnitude, which is also more or less anticipated, as NCD stems from the chiral positioning of the NPs in space. By inserting the gold core inside the cobalt-NP helices, the rotation angles and all corresponding dichroism spectra are greatly enhanced similarly to the magnetite nanohelices. As witnessed from Figure 5, the rotation angles (see Figure 5a) increase by more than 2 orders magnitude, NCD by 2, MCD by 1, and MChD by 4 orders of magnitude. By comparing Figure 3 for magnetite nanohelices@gold nanorods with Figure 5, i.e., cobalt nanohelices@gold nanorods, we observe that NCD curves are more or less the same, signifying the role of the gold nanorod in this type of circular dichroism. Namely, although the NCD for cobalt-NP helices without the gold core is about double the NCD for magnetite-NP helices (without the gold core), with the insertion of the gold core, the excitation of the corresponding surface plasmon resonances of the gold core (see Figure S1 of the Supporting Information) boosts the NCD spectra, leaving in the background the differences arising from the dissimilar dielectric functions of cobalt and magnetite (differences that are evident by comparing Figure 2b and Figure 4b, i.e., in the absence of the gold core). The MCD spectra for the cobalt nanohelices@gold nanorods (Figure 5c) are about 50% increased relative to the corresponding MCD of magnetite nanohelices@gold nanorods due to the larger MO (off-diagonal) components (Voigt parameter) of the dielectric tensor of bulk cobalt (see Figure S3 of the Supporting Information). However, by comparing the MChD spectra of

DOI: 10.1021/acsphotonics.5b00237
ACS Photonics 2015, 2, 1030−1038

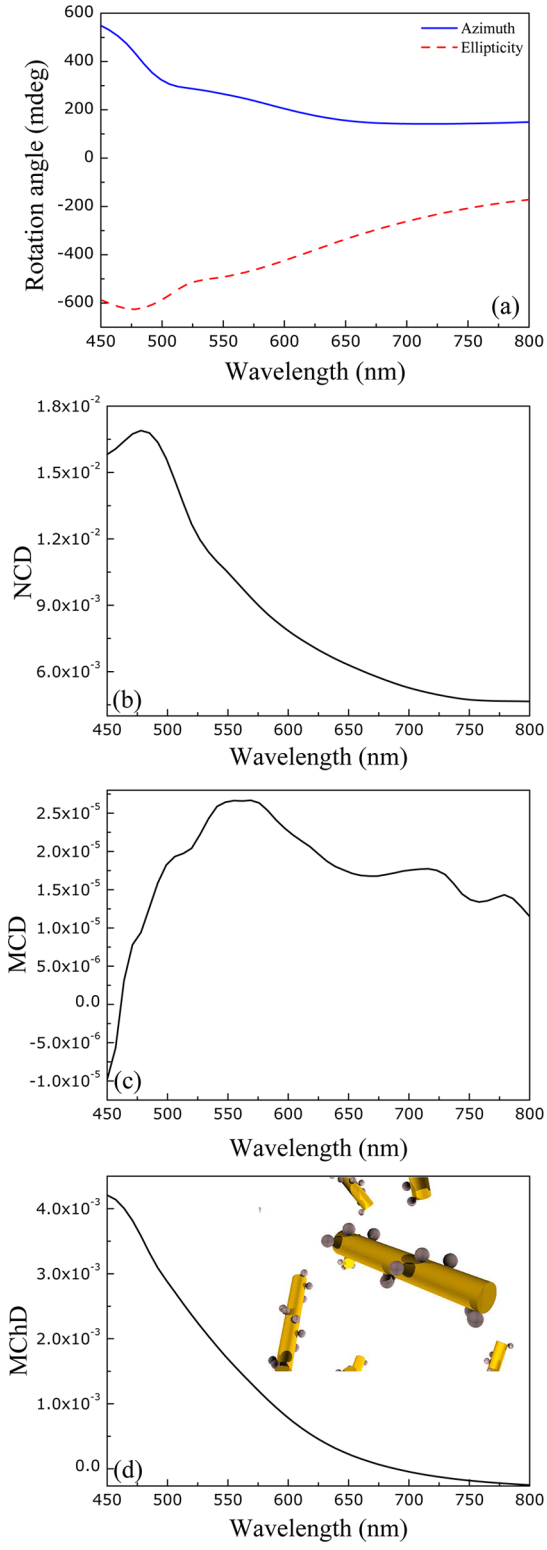

Figure 3. (a) Azimuth and ellipticity rotation angle for light incident along the positive z-axis at a suspension of 5 nm magnetite nanospheres forming helices coiled two times around a gold cylinder with height h = 140 nm and diameter d = 10 nm; that is, the solution consists of mangetite NP helices@nanorods (see inset of part d) with volume density f = 0.5%. (b) Spectrum of natural dichroism (zero magnetic field) NCD. (c and d) Corresponding spectra for the magnetic (MCD) and magnetochiral (MChD) dichroism, respectively, for a magnetic field of 0.5 T along the positive z-axis.

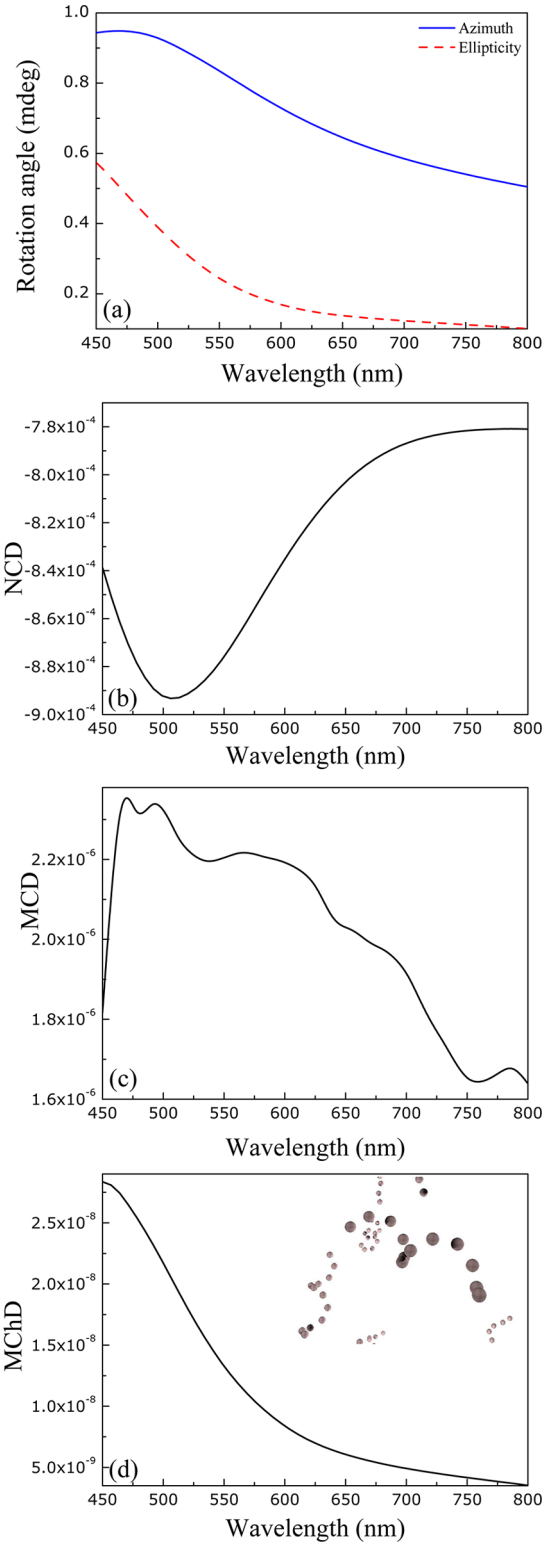

Figure 4. The same as Figure 2 but for cobalt NPs.

Figure 3d and Figure 5d, we observe that the MChD for the magnetite nanohelices is more than 1 order of magnitude higher than the MChD for the cobalt ones. This is not an anticipated result since the MChD is usually interpreted as a cross-effect (see above) that is enhanced by the simultaneous presence of structural (NCD) and magnetic (MCD) chirality. Namely, as structural chirality, NCD, is practically the same for both magnetite and cobalt nanohelices (see above) and MCD is

DOI: 10.1021/acsphotonics.5b00237
ACS Photonics 2015, 2, 1030−1038

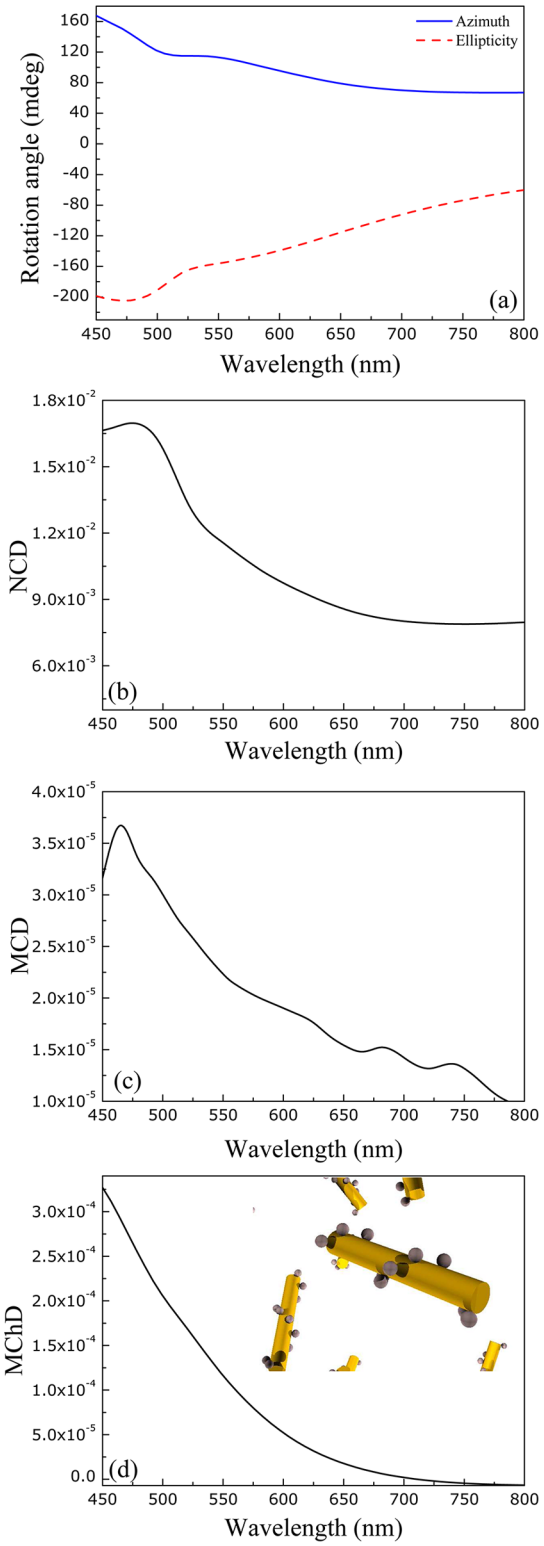

Figure 5. The same as Figure 3 but for cobalt NPs.

more pronounced for cobalt nanohelices, MChD is expected to be likewise more enhanced in cobalt nanohelices than in the magnetite ones.

In order to make a more in-depth exploration of the above counterintuitive phenomenon, in Figure 6 we show the spectrum of the product of (NCD) × (MCD) for both types of nanohelices to be compared with that of MChD. Evidently, there is a discrepancy between these quantities: although the

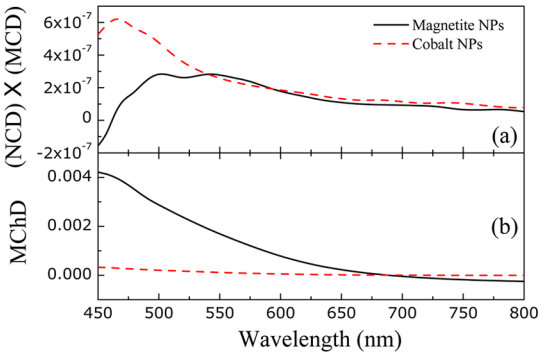

Figure 6. Spectrum of the product (NCD) × (MCD) (a) and of the MChD (b) for magnetoplasmonic helices of magnetite (solid) and cobalt (broken) NPs.

cobalt nanohelices exhibit a much larger product (NCD) × (MCD) than the magnetite ones, the MChD is larger (at short wavelengths significantly larger) for the magnetite rather than the cobalt ones. This discrepancy is a demonstration of the so-called *pure* MChD being distinct from the *cascaded* MChD associated with the product (NCD) × (MCD).[3] A pure MChD effect has been recently demonstrated experimentally in chiral nanomagnets.[15] As stated above, the condition under which the MChD is explained as a cascade effect of NCD and MCD is where the real parts of the dielectric tensor elements are much larger than the corresponding imaginary parts. By inspecting the elements of the dielectric tensor of both cobalt and magnetite (see Figures S2 and S3 of the Supporting Information) it is evident that such a condition is not satisfied especially for magnetite.

The emergence of a pure MChD effect partly explains the larger MChD in the magnetite nanohelices compared to the cobalt ones since it is not necessary to have enhanced MCD to observe a similarly enhanced MChD. In reality, besides MChD, there may be other mechanisms behind the observed reciprocity-violating anisotropy, i.e., the fact that light beams propagating at opposite directions experience different absorption rates. Such a mechanism is the presence of a toroidal moment $\mathbf{T}$ in the material system.[65] This toroidal moment may appear in the form of a ferrotoroidic moment in multiferroic materials[9,11,12] where $\mathbf{T} = \mathbf{P} \times \mathbf{M}$, with $\mathbf{P}$ and $\mathbf{M}$ being the spontaneous polarization and magnetization, respectively. However, it may also appear in the form of an induced toroidal moment, where electric $\mathbf{p}$ and magnetic $\mathbf{m}$ dipole moments may emerge simultaneously from external fields or incident light,[65] as is the case in, for example, toroidal metamaterials.[66−69] In this respect, we have calculated the toroidal moment $\mathbf{T} = \mathbf{p}_{rod} \times \mathbf{m}_{hel}$ for a *single* nanohelix@gold nanorod, where $\mathbf{p}_{rod}$ is the electric-dipole moment of the gold nanorod and $\mathbf{m}_{hel}$ the magnetic-dipole moment of the magnetite or cobalt nanohelix. In Figure 7 we show the average $\mathbf{T}$ over 10 different orientations of the nanohelix@nanorod when the magnetic field is staggered along the *z*-axis (broken lines) and when the magnetic field is parallel to the (random) orientations of the gold nanorod. Evidently, there is a large difference in the toroidal moment between the magnetite and cobalt nanohelices, which may explain the observed magnetochiral anisotropy. Namely, the presence of toroidal moment $\mathbf{T}$ in a medium induces a change in the dielectric function of the type

DOI: 10.1021/acsphotonics.5b00237
ACS Photonics 2015, 2, 1030−1038

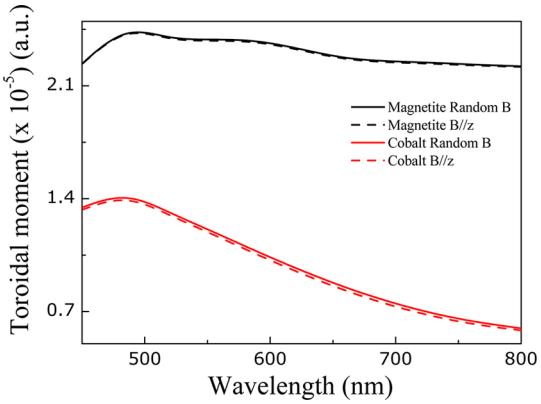

Figure 7. Spectrum of the toroidal moment of a single magnetite@gold and cobalt@gold nanohelix averaged over 10 different (random) helix orientations (orientational average). For the solid lines, the external magnetic field **B** is generally randomly oriented in space, being parallel to the particular axis of the helix. For the broken lines the magnetic field **B** is staggered along the *z*-axis (as in Figures 1−6).

$$\Delta\epsilon = \eta_{\text{toroid}}^{\text{L,R}}(\omega)\mathbf{k}\cdot\mathbf{T} \tag{6}$$

which is similar to the magnetochiral contribution of eq 1; that is, it introduces a dependence of the dielectric function on whether the propagation direction is parallel or antiparallel to the toroidal moment **T**, leading to nonreciprocal propagation.[70]

Currently, there is no effective-medium theory, to the best of our knowledge, which may provide a formula for $\eta_{\text{toroid}}^{\text{L,R}}$ and create a more concrete basis for the contribution of the toroidal moment to the observed MChD. It is worth noting that, to the apparent increase of the toroidal moment **T** also contributes the electric-dipole moment $\mathbf{p}_{\text{rod}}$ of the gold nanorod as a result of the surface-plasmon excitation at short wavelengths (see Figure S1 of the Supporting Information), especially the low-frequency plasmon, which oscillates normal to the rod axis and thus to the magnetic moment of the helix. Note, in passing, that the magnetic-dipole moment $\mathbf{m}_{\text{hel}}$ involved in the calculated toroidal moment **T** stems from the current flowing along a helix as a result of the electric (near-field) coupling of the NPs and not by the magnetic-dipole moment of each individual magnetic (magnetite or cobalt) NP, which is irrelevant in the optical regime (this is also demonstrated by the coincidence of the solid and broken lines in Figure 7). The above current contains also a nonreciprocal component stemming from the off-diagonal part (Figure S3) of the dielectric tensor and gives rise to a corresponding nonreciprocal component of **T**.

In order to shine more light on the difference of the MChD between the magnetite and cobalt nanohelices, in Figure 8 we compare the MChD of a collection of nanohelices@nanorods when the magnetic field is steadily parallel to the *z*-axis (broken lines) with the MChD curve when the magnetic field assumes the (random) orientation direction of each nanohelix (solid lines). Evidently, there is a dramatically different behavior between the magnetite and cobalt nanohelices. For magnetite helices both curves practically coincide, whereas for the cobalt nanohelices the randomness in the magnetic field direction reduces the MChD by more than 5 orders of magnitude. It appears that the MChD in cobalt nanohelices is a collective phenomenon with strong interaction between the nanohelices@nanorods within the solution, whereas the MChD phenomenon for the magnetite nanohelices stems from the response of the isolated nanohelix@nanorod. The strongest

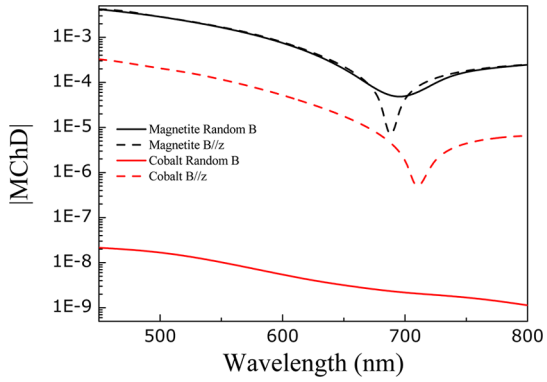

Figure 8. Broken lines: MChD spectra of Figure 6b. Solid lines: MChD spectra when the external magnetic field **B** is generally randomly oriented in space, being parallel to the particular axis of the helix.

interaction among the cobalt nanohelices is a result of the negative values of the diagonal part of the corresponding dielectric tensor (see Figure S2 of the Supporting Information), which imparts a metallic behavior to the cobalt NPs, resulting in a stronger multiple scattering of incident radiation and subsequently a stronger coupling among the nanohelices. From the above discussion on the toroidal moment of a single nanohelix@nanorod along with the discussion on the dependence of the MChD on the orientation of the applied magnetic field, we may speculate that the observed departure of the MChD from the combined NCD/MCD cascade effect lies in the emergence of a surface-plasmon-induced toroidal moment at each *individual* nanohelix@nanorod. The latter phenomenon is more pronounced in the magnetite helices than in the cobalt ones, leading to larger MChD in the magnetite case.

Finally, in Figure 9 we examine the effect of density on the MChD for the case of magnetite helices@gold nanorods. We

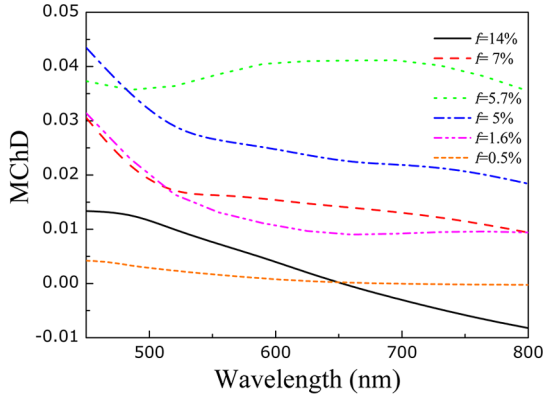

Figure 9. Magnetochiral dichroism (MChD) for a suspension of magnetite@gold nanohelices for different values of the volume filling fraction *f* as shown in the legend. The magnetic field **B** is along the *z*-axis.

observe that MChD is *not* a monotonic function of the density (in the caption of Figure 9 we write down explicitly the volume filling fraction covered by the NPs and the nanorods). It seems that the MChD saturates up to about $f = 6\%$, and beyond this value it starts to decrease with increasing packing fraction (density). As has been already pointed out,[71] the dense NP packing does not favor strong enhancement of the chiral dishroism because of the weaker field concentration within the

DOI: 10.1021/acsphotonics.5b00237
ACS Photonics 2015, 2, 1030−1038

NPs as a result of the stronger interaction among the SP modes of the gold nanorods.

We note that for high packing fractions (f > 10%) the helices@nanorods are not completely randomly oriented in space but start to point (with fluctuations) in a particular direction in space resembling the molecular conformations in a nematic liquid crystal. Obviously, the suspension attains a uniaxial EM response in which case eq 1 needs to be generalized for a general anisotropic case.[3]

CONCLUSION

We have demonstrated theoretically that dilute suspensions of helices of magnetite or cobalt NPs coiled around a gold core exhibit strong magnetochiral/magneto-optical dichroism and Faraday rotation over broad spectral regions due to the excitation of gold SPs at the gold cores, which localize the electric field within subwavelength volumes and enhance drastically the magneto-optical effect and, in turn, the magnetochirality. However, we have shown that despite the great enhancement of the magneto-optical effect, the observed magnetochiral dichroism is not a cascading of structural and magnetic dichroism but is possibly attributed to a surface-plasmon-induced toroidal moment generated within the individual nanohelices. This is the first time, to the best of our knowledge, that the emergence of a toroidal moment in a material can show significant reciprocity-violating anisotropy in the visible regime. Suspensions of magnetic nanohelices@gold cores can be realized in the laboratory by bottom-up processes such as supramolecular self-assembly as well as peptide- and DNA-assisted self-assembly, which both are much easier means to produce magnetoplasmonic metamaterials than traditional lithographic techniques.

ASSOCIATED CONTENT

Supporting Information

In the Supporting Information we outline the theory (DDA) for the calculation of the various types of circular dichroism. We also provide the spectrum of the scattering cross section for a single gold nanorod as well as the spectra of the diagonal and off-diagonal elements of the dielectric tensors for magnetite and cobalt. The Supporting Information is available free of charge on the ACS Publications website at DOI: 10.1021/acsphotonics.5b00237.

AUTHOR INFORMATION

Corresponding Author

*E-mail: vyannop@mail.ntua.gr.

Notes

The authors declare no competing financial interest.

REFERENCES

(1) Landau, L. D.; Lifshitz, E. M. *Electrodynamics of Continuous Media*; Pergamon: Oxford, 1984.
(2) Rikken, G. L. J. A.; Raupach, E. Observation of magneto-chiral dichroism. *Nature (London, U. K.)* **1997**, *390*, 493−494.
(3) Rikken, G. L. J. A.; Raupach, E. Pure and cascaded magnetochiral anisotropy in optical absorption. *Phys. Rev. E: Stat. Phys., Plasmas, Fluids, Relat. Interdiscip. Top.* **1998**, *58*, 5081−5084.
(4) Kleindienst, P.; Wagnière, G. H. Inteferometric detection of magnetochiral birefringence. *Chem. Phys. Lett.* **1998**, *288*, 89−97.
(5) Kalugin, N. G.; Kleindinst, P.; Wagnière, G. H. The magneto-chiral birefirngence in diamagnetic solutions and in uniaxial crystals. *Chem. Phys.* **1999**, *248*, 105−115.
(6) Rikken, G. L. J. A.; Raupach, E. Enantioselective magnetochiral photochemistry. *Nature (London, U. K.)* **2000**, *405*, 932−935.
(7) Vallet, M.; Ghosh, R.; le Floch, A.; Ruchon, T.; Bretenaker, F.; Thépot, J. Y. Observation of magnetochiral birefringence. *Phys. Rev. Lett.* **2001**, *87*, 183003.
(8) Saito, M.; Ishikawa, K.; Taniguchi, K.; Arima, T. Magnetic control of crystal chirality and the existence of a large magneto-optical dichroism effect in CuB_2O_4. *Phys. Rev. Lett.* **2008**, *101*, 117402.
(9) Train, C.; Gheorghe, R.; Krstic, V.; Chamoreau, L. M.; Ovanesyan, N. S.; Rikken, G. L. J. A.; Gruselle, M.; Verdaguer, M. Strong magneto-chiral dichroism in enantiopure chiral ferromagnets. *Nat. Mater.* **2008**, *7*, 729−734.
(10) Kitagawa, Y.; Segawa, H.; Ishii, K. Magneto-chiral dichroism of orgranic compounds. *Angew. Chem., Int. Ed.* **2011**, *50*, 9133−9136.
(11) Miyahara, S.; Furukawa, N. Nonreciprocal directional dichroism and toroidalmagnons in helical magnets. *J. Phys. Soc. Jpn.* **2012**, *81*, 023712.
(12) Kibayashi, S.; Takahashi, Y.; Seki, S.; Tokura, Y. Magnetochiral dichroism resonant with electromagnons in a helimagnet. *Nat. Commun.* **2014**, *5*, 4583.
(13) Sessoli, R.; Boulon, M. E.; Caneschi, A.; Mannini, M.; Poggini, L.; Wilhelm, F.; Rogalev, A. Strong magneto-chiral dichroism in a paramagnetic molecular helix observed by hard X-rays. *Nat. Phys.* **2015**, *11*, 69−74.
(14) Christofi, A.; Stefanou, N. Strong magnetochiral dichroism of helical structures of garnet particles. *Opt. Lett.* **2013**, *38*, 4629−4631.
(15) Eslami, S.; Gibbs, J. G.; Rechkemmer, Y.; van Slageren, J.; Alarcón-Correa, M.; Lee, T. C.; Mark, A. G.; Rikken, G. L. J. A.; Fischer, P. Chiral nanomagnets. *ACS Photonics* **2014**, *1*, 1231−1236.
(16) Li, Y.; Zhang, Q.; Nurmikko, A. V.; Sun, S. Enhanced magnetooptical response in dumbbell-like Ag−$CoFe_2O_4$ nanoparticle pairs. *Nano Lett.* **2005**, *5*, 1689−1692.
(17) González-Díaz, J. B.; García-Martín, A.; García-Martín, J. M.; Cebollada, A.; Armelles, G.; Sepúlveda, B.; Alaverdyan, Y.; Käll, M. Plasmonic Au/Co/Au nanosandwiches with enhanced magneto-optical activity. *Small* **2008**, *4*, 202−205.
(18) Armelles, G.; González-Díaz, J. B.; García-Martín, A.; García-Martín, J. M.; Cebollada, A.; González, M. U.; Acimovic, S.; Cesario, J.; Quidant, R.; Badenes, G. Localized surface plasmon resonance effects on the magneto-optical activity of continuous Au/Co/Au trilayers. *Opt. Express* **2008**, *16*, 16104−16112.
(19) Moolekamp, F. E.; Stokes, K. L. Magnetooptical response of gold-magnetite nanocomposite films. *IEEE Trans. Magn.* **2009**, *45*, 4888−4891.
(20) Jain, P. K.; Xiao, Y.; Walsworth, R.; Cohen, A. E. Surface plasmon resonance enhanced magneto-optics (SuPREMO): Faraday rotation enhancement in gold-coated iron oxide nanocrystals. *Nano Lett.* **2009**, *9*, 1644−1650.
(21) González-Díaz, J. B.; Sepúlveda, B.; García-Martín, A.; Armelles, G. Cobalt dependence of the magneto-optical response in magneto-plasmonic nanodisks. *Appl. Phys. Lett.* **2010**, *97*, 043114.
(22) Du, G. X.; Mori, T.; Suzuki, M.; Saito, S.; Fukuda, H.; Takahashi, M. Evidence of localized surface plasmon enhanced magneto-optical effect in nanodisk array. *Appl. Phys. Lett.* **2010**, *96*, 081915.
(23) Du, G. X.; Mori, T.; Saito, S.; Takahashi, M. Shape-enhanced magneto-optical activity: Degree of freedom for active plasmonics. *Phys. Rev. B: Condens. Matter Mater. Phys.* **2010**, *82*, 1614039(R).
(24) Demidenko, Y.; Makarov, D.; Lozovski, V. Local-field effects in magneto-plasmonic nanocomposites. *J. Opt. Soc. Am. B* **2010**, *27*, 2700−2706.
(25) Dani, R. K.; Wang, H.; Bossmann, S. H.; Wysin, G.; Chikan, V. Faraday rotation enhancement of gold coated Fe_2O_3 nanoparticles: Comparison of experiment and theory. *J. Chem. Phys.* **2011**, *135*, 224502.
(26) Wang, L.; Clavero, C.; Huba, Z.; Caroll, K. J.; Carpenter, E. E.; Gu, D.; Lukaszew, R. A. Plasmonics and enhanced magneto-optics in core-shell Co-Ag nanoparticles. *Nano Lett.* **2011**, *11*, 1237−1240.

DOI: 10.1021/acsphotonics.5b00237
ACS Photonics 2015, 2, 1030−1038

(27) Du, G. X.; Saito, S.; Takahashi, M. Tailoring the Faraday effect by birefringence of two dimensional plasmonic nanorod array. *Appl. Phys. Lett.* **2011**, *99*, 191107.
(28) Valev, V. K.; Silhanek, A. V.; Gillijns, W.; Jeyaram, Y.; Paddubrouskaya, H.; Volodin, A.; Biris, C. G.; Panoiu, N. C.; de Clercq, B.; Ameloot, M.; Aktsipetrov, O. A.; Moshchalkov, V. V.; Verbiest, T. Plasmons reveal the direction of magnetization in nickel nanostructures. *ACS Nano* **2011**, *5*, 91−96.
(29) Armelles, G.; Cebollada, A.; García-Martín, A.; Montero-Moreno, J. M.; Waleczek, M.; Nielsch, K. Magneto-optical properties of core-shell magneto-plasmonic $AuCo_xFe_{3-x}O_4$ nanowires. *Langmuir* **2012**, *28*, 9127−9130.
(30) Pakdel, S.; Miri, M. Faraday rotation and circular dichroism spectra of gold and silver nanoparticle aggregates. *Phys. Rev. B: Condens. Matter Mater. Phys.* **2012**, *86*, 235445.
(31) Armelles, G.; Cebollada, A.; García-Martín, A.; González, M. U. Magnetoplasmonics: Combining Magnetic and Plasmonic Functionalities. *Adv. Opt. Mater.* **2013**, *1*, 10−35.
(32) Christofi, A.; Stefanou, N. Nonreciprocal optical response of helical periodic structures of plasma spheres in a static magnetic field. *Phys. Rev. B: Condens. Matter Mater. Phys.* **2013**, *87*, 115125.
(33) Christofi, A.; Stefanou, N. Nonreciprocal photonic surface states in periodic structures of magnetized plasma nanospheres. *Phys. Rev. B: Condens. Matter Mater. Phys.* **2013**, *88*, 125133.
(34) Nahal, A.; Talebi, R. Ellipticity-dependent laser-induced optical gyrotropy in AgCl thin films doped by silver nanoparticles. *J. Nanopart. Res.* **2014**, *16*, 2442.
(35) Armelles, G.; Caballero, B.; Cebollada, A.; García-Martín, A.; Meneses-Rodríguez, D. Magnetic field modification of optical magnetic dipoles. *Nano Lett.* **2015**, *15*, 2045−2049.
(36) Fan, J. A.; Wu, C.; Bao, K.; Bao, J.; Bardhan, R.; Halas, N. J.; Manoharan, V. N.; Nordlander, P.; Shvets, G.; Capasso, F. Self-assembled plasmonic nanoparticle clusters. *Science* **2010**, *328*, 1135−1138.
(37) Oh, H. S.; Jee, H.; Baev, A.; Swihart, M. T.; Prasad, P. N. Chiral poly(fluorene-alt-benzothiadiazole) (PFBT) and nanocomposites with gold nanoparticles: plasmonically and structurally enhanced chirality. *J. Am. Chem. Soc.* **2010**, *132*, 17346−17348.
(38) Jones, M. R.; Osberg, K. D.; Macfarlane, R. J.; Langille, M. R.; Mirkin, C. A. Templated techniques for the synthesis and assembly of plasmonic nanostructures. *Chem. Rev.* **2011**, *111*, 3736−3827.
(39) Mastroianni, A. J.; Claridge, S. A.; Alivisatos, A. P. Pyramidal and chiral groupings of gold nanocrystals assembled using DNA scaffolds. *J. Am. Chem. Soc.* **2009**, *131*, 8455−8459.
(40) Sharma, J.; Chhabra, R.; Cheng, A.; Brownell, J.; Liu, Y.; Yan, H. Control of self-assembly of DNA tubules through integration of gold nanoparticles. *Science* **2009**, *323*, 112−116.
(41) Tan, S. J.; Campolongo, M. J.; Luo, D.; Cheng, W. Building plasmonic nanostructures with DNA. *Nat. Nanotechnol.* **2011**, *6*, 268−276.
(42) Slocik, J. M.; Govorov, A. O.; Naik, R. R. Plasmonic circular dichroism of peptide-functionalized gold nanoparticles. *Nano Lett.* **2011**, *11*, 701−705.
(43) Shen, X.; Song, C.; Wang, J.; Shi, D.; Wang, Z.; Liu, N.; Ding, B. Rolling up gold nanoparticle-dressed DNA origami into three-dimensional plasmonic chiral nanostructures. *J. Am. Chem. Soc.* **2012**, *134*, 146−149.
(44) Kuzyk, A.; Schreiber, R.; Fan, Z.; Pardatscher, G.; Roller, E. M.; Högele, A.; Simmel, F. C.; Govorov, A. O.; Liedl, T. DNA-based self-assembly of chiral plasmonic nanostructures with tailored optical response. *Nature* **2012**, *483*, 311−314.
(45) Yannopapas, V. Negative index of refraction in artificial chiral materials. *J. Phys.: Condens. Matter* **2006**, *18*, 6883−6890.
(46) Fan, Z.; Govorov, A. O. Plasmonic circular dichroism of chiral metal nanoparticle assemblies. *Nano Lett.* **2010**, *10*, 2580−2587.
(47) Fan, Z.; Govorov, A. O. Helical metal nanoparticle assemblies with defects: Plasmonic chirality and circular dichroism. *J. Phys. Chem. C* **2011**, *115*, 13254−13261.
(48) Guerrero-Martínez, A.; Auguié, B.; Alonso-Gómez, J. L.; Džolić, Z.; Gómez-Graña, S.; Žinić, M.; Cid, M. M.; Liz- Marzán, L. M. Intense optical activity from three-dimensional chiral ordering of plasmonic nanoantennas. *Angew. Chem., Int. Ed.* **2011**, *50*, 5499−5503.
(49) Guerrero-Martínez, A.; Alonso-Gómez, J. L.; Auguié, B.; Cid, M. M.; Liz- Marzán, L. M. From individual to collective chirality in metal nanoparticles. *Nano Today* **2011**, *6*, 381−400.
(50) Gao, W.; Leung, H. M.; Li, Y.; Chen, H.; Tam, W. Y. Circular dichroism in double-layer metallic crossed-gratings. *J. Opt.* **2011**, *13*, 115101.
(51) Hentschel, M.; Schäferling, M.; Weiss, T.; Liu, N.; Giessen, H. Three-dimensional chiral plasmonic oligomers. *Nano Lett.* **2012**, *12*, 2542−2547.
(52) Zhao, Y.; Belkin, M. A.; Alú, A. Twisted optical metamaterials for planarized ultrathin broadband circular polarizers. *Nat. Commun.* **2012**, *3*, 870.
(53) Christofi, A.; Stefanou, N.; Gantzounis, G.; Papanikolaou, N. Spiral-staircase photonic structures of metallic nanorods. *Phys. Rev. B: Condens. Matter Mater. Phys.* **2012**, *84*, 125109.
(54) Christofi, A.; Stefanou, N.; Gantzounis, G.; Papanikolaou, N. Giant optical activity of helical architectures of plasmonic nanorods. *J. Phys. Chem. C* **2012**, *116*, 16674−16679.
(55) Droulias, S.; Yannopapas, V. Broad-band giant circular dichroism in metamaterials of twisted chains of metallic nanoparticles. *J. Phys. Chem. C* **2013**, *117*, 1130−1135.
(56) Draine, B. T. The discrete-dipole approximation and its application to stellar graphite grains. *Astrophys. J.* **1988**, *333*, 848−872.
(57) Draine, B. T.; Flatau, P. J. Discrete-dipole approximation for scattering calculations. *J. Opt. Soc. Am. A* **1994**, *11*, 1491−1499.
(58) Yurkin, M. A.; Hoekstra, A. G. The discrete dipole approximation: an overview and recent developments. *J. Quant. Spectrosc. Radiat. Transfer* **2007**, *106*, 558−589.
(59) Smith, D. A.; Barnakov, Y. A.; Scott, B. L.; White, S. A.; Stokes, K. L. Magneto-optical spectra of closely-spaced magnetite nanoparticles. *J. Appl. Phys.* **2005**, *97*, 10M504.
(60) Smith, D. A.; Stokes, K. L. Discrete dipole approximation for magnetooptical scattering calculations. *Opt. Express* **2006**, *14*, 5746−5754.
(61) Schlegel, A.; Alvarado, S. F.; Wachter, P. Optical properties of magnetite (Fe_3O_4). *J. Phys. C: Solid State Phys.* **1979**, *12*, 1157−1164.
(62) Zhang, X.; Schoenes, J.; Wachter, P. Kerr-effect and dielecric tensor elements of magnetite (Fe_3O_4) between 0.5 and 4.3 eV. *Solid State Commun.* **1981**, *39*, 189−192.
(63) Meneses-Rodríguez, D.; Ferreiro-Vila, E.; Prieto, P.; Anguita, J.; González, M. U.; García-Martin, J. M.; Cebollada, A.; García-Martin, A.; Armelles, G. Probing the electromagnetic field distribution within a metallic nanodisk. *Small* **2011**, *7*, 3317−3323.
(64) Armelles, G.; Caballero, B.; Prieto, P.; García, F.; González, M. U.; García-Martin, A.; Cebollada, A. Magnetic field modulation of chirooptical effects in magnetoplasmonic structures. *Nanoscale* **2014**, *6*, 3737−3741.
(65) Szaller, D.; Bordács, S.; Kézsmárki, I. Symmetry conditions for nonreciprocal light propagation in magnetic crystals. *Phys. Rev. B: Condens. Matter Mater. Phys.* **2013**, *87*, 014421.
(66) Papasimakis, N.; Fedotov, V. A.; Marinov, K.; Zheludev, N. I. Gyrotropy of a metamolecule: wire on a torus. *Phys. Rev. Lett.* **2009**, *103*, 093901.
(67) Kaelberer, T.; Fedotov, V. A.; Papasimakis, N.; Tsai, D. P.; Zheludev, N. I. Toroidal dipolar response in a metamaterial. *Science* **2010**, *330*, 1510.
(68) Dong, Z. G.; Zhu, J.; Yin, X.; Li, J.; Lu, C.; Zhang, X. All-optical Hall effect by the dynamic toroidal moment in a cavity-based metamaterial. *Phys. Rev. B: Condens. Matter Mater. Phys.* **2013**, *87*, 245429.
(69) Basharin, A. A.; Kafesaki, M.; Economou, E. N.; Soukoulis, C. M.; Fedotov, V. A.; Savinov, V.; Zheludev, N. I. Dielectric metamaterials with toroidal dipolar response. *Phys. Rev. X* **2015**, *5*, 011036.

DOI: 10.1021/acsphotonics.5b00237
ACS Photonics 2015, 2, 1030−1038

(70) Sawada, K.; Nagaosa, N. Optical magnetoelectric effect in multiferroic materials: evidence for a Lorentz force acting on a ray of light. *Phys. Rev. Lett.* **2005**, *95*, 237402.
(71) Christofi, A.; Stefanou, N.; Papanikolaou, N. Periodic structures of magnetic garnet particles for strong Faraday rotation enhancement. *Phys. Rev. B: Condens. Matter Mater. Phys.* **2014**, *89*, 214410.

DOI: 10.1021/acsphotonics.5b00237
ACS Photonics 2015, 2, 1030−1038